

---

ATTI ACCADEMIA NAZIONALE DEI LINCEI  
CLASSE SCIENZE FISICHE MATEMATICHE NATURALI  
**RENDICONTI**

---

CLAUDIO EBBLIN

**Structural Geology of the Thalle Area, Baltistan,  
Karakorum, Central Asia. Nota II**

*Atti della Accademia Nazionale dei Lincei. Classe di Scienze Fisiche,  
Matematiche e Naturali. Rendiconti, Serie 8, Vol. 60 (1976), n.6, p. 853–857.*

Accademia Nazionale dei Lincei

<[http://www.bdim.eu/item?id=RLINA\\_1976\\_8\\_60\\_6\\_853\\_0](http://www.bdim.eu/item?id=RLINA_1976_8_60_6_853_0)>

L'utilizzo e la stampa di questo documento digitale è consentito liberamente per motivi di ricerca e studio. Non è consentito l'utilizzo dello stesso per motivi commerciali. Tutte le copie di questo documento devono riportare questo avvertimento.

---

*Articolo digitalizzato nel quadro del programma  
bdim (Biblioteca Digitale Italiana di Matematica)  
SIMAI & UMI*

<http://www.bdim.eu/>



**Geologia.** — *Structural Geology of the Thalle Area, Baltistan, Karakorum, Central Asia.* Nota II di CLAUDIO EBBLIN, presentata (\*) dal Socio A. DESIO.

RIASSUNTO. — Le strutture geologiche dell'area di Thalle a NE del villaggio di Skardu nel Pakistan settentrionale, rivelano la presenza delle tracce di piani assiali di varie pieghe di primo ordine. Tali pieghe appartengono a due generazioni differenti e si sono quindi formate durante due distinte fasi di deformazione. Le più antiche sembrano essere connesse con la formazione del Batolite assiale del Karakorum e le più recenti con i probabili assestamenti dovuti all'accavallamento di rocce del basamento su quelle della copertura. La successiva intrusione di una massa di gabbrodiorite è stata anche messa in evidenza.

### 3. CONCLUSIONS

#### 3.1. *Structural reconstruction.*

Two different cleavages can be distinguished in the area; one is a schistosity generally parallel to the compositional banding but placed at an angle to it in the hinge zone of early folds, and the other is a cleavage which takes the form of a crenulation in the mica-rich rocks and of a fracture cleavage in the more quartzofeldspathic ones. Obviously the schistosity which is the oldest of the two might have destroyed earlier features, traces of which are no longer detectable. Thus the chronological sequence of formation of planar elements in the rocks is: compositional banding (*ss*) first, schistosity (*S*<sub>1</sub>) second and crenulation cleavage or fracture cleavage (*S*<sub>2</sub>) third. All shear fractures or joints were not taken into consideration, their genetical interpretation being a much more controversial matter.

In order to attempt a reconstruction of the orientation of the principal axes of finite strain of the different deformational stages undergone by the rocks of the area the effects of the (*F*<sub>2</sub>) youngest deformation will be examined first.

The orientation of the *S*<sub>2</sub> cleavages (fig. 5) considered to be perpendicular to the direction of maximum finite shortening of the *F*<sub>2</sub> deformational event is quite constant across the area. Thus the direction of maximum shortening can be assumed to have occurred in a subvertical direction. However the stereogram shows that the *S*<sub>2</sub> is parallel to a cylindrical surface, the axis of which is subhorizontal in the ENE direction thus showing that the *F*<sub>2</sub> deformational stage was followed by yet a younger stage.

The spatial relationships between the schistosity and the crenulation cleavage in the upper Thalle Valley (fig. 6) show that the former has been folded by the latter about SE-plunging axes. Furthermore, the distribution of poles to the compositional banding (fig. 7) reveals that these surfaces are conically folded about NE-plunging axes.

(\*) Nella seduta dell'8 maggio 1976.

Conical folds of the compositional banding can be the result either of interference of subsequent stages of cylindrical folding or of bending around bodies showing a subcircular horizontal section. In order to produce the above-mentioned interference effect the direction of maximum shortening of the latter deformational stage must be at less than  $45^\circ$  from the axis of folding of the former stage. Thus F1 ought to have been followed by a deformational phase with southeasterly maximum shortening. However no traces of such a phase were found in the area and thus the alternative interpretation was preferred.

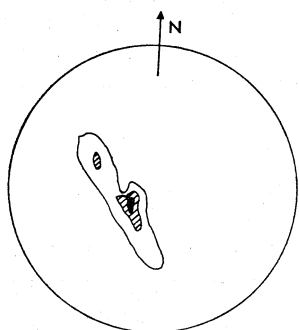


Fig. 5. - Stereogram representing the poles of the crenulation cleavages; 12 measurements. Density: 8%, 16%, 25%. Projection on an equal-area net, lower hemisphere.

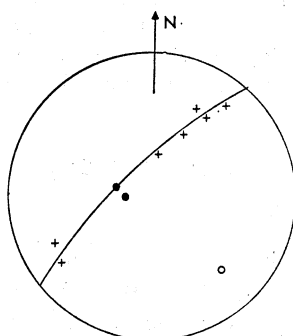


Fig. 6. - Stereogram representing the poles to the cleavages. Crosses: schistosity; full circles: crenulation cleavages; open circle:  $\beta$ -axis of crenulation folds. Lower hemisphere.

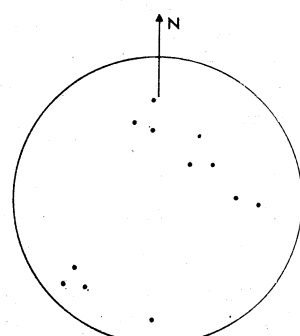


Fig. 7. - Stereogram representing the poles to the compositional banding. Lower hemisphere.

A deformational history of the area can be thus summarized as follows.

The oldest F1 deformational phase detected in the area yielded NE-SW maximum finite shortening and folding about subhorizontal axes. The main schistosity formed parallel to the axial surfaces of these folds. The following F2 deformational event with its axis of maximum finite contraction dipping very steeply to the west must have occurred along with the formation of the crenulation cleavage and the fracture cleavage.

Finally, the gabbrodioritic body was emplaced along the regional schistosity while a new schistosity might have formed in the vicinity of the igneous complex.

The planar S2 was bent slightly about NE-plunging axes while the S1, due to its different orientation, was bent about the already-existing SE-plunging axes. The shape of the folds of the compositional banding was instead modified from cylindrical to conical.

#### 4. CORRELATIONS WITH THE SURROUNDING AREAS

The basic igneous complex constituting the peaks of the Shimshak is made of rocks which ought to be very similar to the dioritic gneisses of the Skoro Pass that in turn much resemble (Zanettin, 1964) the rocks

observed along the Twar Valley. Hence the complex might be considered to be a body of Twar Diorite (Desio, 1964).

The volcano-sedimentary sequence was thought (Zanettin, 1964) to be a lateral variation of the Cretaceous labradoritic gneisses and perhaps also of the overlying limestones visible on the eastern slope of the Shigar Valley. However because of compositional similarity it seems more likely that the sequence which makes up the Bauma-Harel Schist of Desio (1964) be the counterpart of the Askore Amphibolite observed further North along the eastern slope of the Shigar Valley. Nevertheless, since the overlying sedimentary sequence corresponds undoubtedly to the Skoro Lumba Slate (Desio, 1964) which has been assumed to belong to the Eocene (Zanettin, 1964), the sequence here appears to be unreversed.

Microscopic evidence from the rocks of the Shigar Valley (Zanettin, 1964) shows that at least three different metamorphic stages can be distinguished there. Indeed traces of an older, probably higher-grade mineral assemblage suggest that the main schistosity is retrograde. Zanettin (1964) concluded that such schistosity was related to the intrusion of the Tisar Tonalite which he considered to be the latest petrogenetic event in the area, subsequent even to the intrusion of the gabbrodioritic bodies. Thus the schistosity observed in the rocks of the Thalle Valley might be older than that of the Shigar Valley.

However even along the Shigar Valley the schistosity appears to be often crenulated and although the orientation of the crenulation cleavage has not been reported, it is likely that it developed at the same time as that in the Thalle Valley. Zones of fresh, recrystallized, polygonal crystals occur along the latter cleavage and appear to be related to it.

On the basis of occurrences of the latter type, Giobbi Mancini (Desio and Giobbi Mancini, 1974) concluded that a phase of static recrystallization followed the latest dynamic phase and related it to the emplacement of the Baltoro Granite which occurred in Miocene time (Desio *et al.*, 1964), perhaps together with that of the gabbrodiorites.

The orientation of the axial surfaces of the F<sub>1</sub> folds in the Thalle area suggests that the folding of the compositional banding about NW-SE axes occurred at the time of the emplacement of the Karakorum Axial Batholith northeast of here. Thus at that time the main regional schistosity ought to have formed. Such a schistosity might have been later replaced by a different younger schistosity locally around the intrusions of igneous rocks.

In the Thalle area the F<sub>1</sub> stage was followed by the F<sub>2</sub> and no evidence of the F<sub>1</sub>-F<sub>2</sub> static phase of recrystallization of Giobbi Mancini (Desio and Giobbi Mancini, 1974) was found.

The schistosity appears to have been distorted by the F<sub>2</sub> deformational stage which seems to be again of regional importance. It is obviously difficult to reconstruct the geological situation connected with a deformation that yielded a maximum finite shortening in a subvertical direction since the revealing elements ought to be found either higher or lower in the

section. However it might be tentatively suggested that here, like further to the northwest in the Yasin-Ishkuman area, the F2 deformation might have been the result of adjustments caused by an excess weight in the overburden (Flinn, 1961). Obviously it remains to be seen whether such an excess weight can be related to the thrusting of the rocks of the basement over those of the cover as seems to be the case in the Yasin-Ishkuman area.

The intrusion of the gabbrodiorite of the Shimshak appears to have followed both the F1 and the F2 deformational stages since the cleavages related to these stages have been bent by the intrusion. Naturally, it is quite likely that the previous existence of the main schistosity has guided the intrusion along surfaces of weakness.

Finally, as an important consequence of the structural reconstruction above, it can be suggested that the Skoyo Gneiss of Desio (1964) might be a higher metamorphic counterpart of the Skoro Lumba Slate.

*Acknowledgments.* The Author is greatly indebted to Prof. A. Desio and to Prof. A. Marussi for introducing him to the problems of the area and for assisting him during the implementation of the project. Thanks are also due to Dr. Giobbi Mancini for helping him with the microscope work and to the staff of the Institute of Geodesy and Geophysics of the University of Trieste who collaborated in many different ways. The Author is also grateful to the Accademia Nazionale dei Lincei and to the Consiglio Nazionale delle Ricerche for their economic support which made the work possible.

## 5. APPENDIX

### LIST OF ROCK SPECIMENS.

- ET 1 *Quartz-biotite-epidote gneiss.* Quartz, feldspar, epidote, opaque, chlorite, muscovite. Medium-grained granular texture, coarser-grained bands of quartz with epidote, unrecrystallized feldspar grains with inclusions of muscovite oriented along two preferential directions.
- ET 2 *Quartz-biotite-epidote gneiss.* Quartz, chlorite, feldspar, opaque, muscovite, epidote. Medium-grained, some elongation of small unrecrystallized quartz and feldspar grains parallel to the compositional banding.
- ET 3 *Quartz-amphibole gneiss.* Quartz, plagioclase, amphibole, epidote. Medium-grained amphibole in three preferential orientations, epidote fine-grained like quartz and plagioclase in bands cross-cutting the compositional banding. Maybe a retrograde recrystallized quartz-diorite.
- ET 4 *Calcareous slate.* Quartz, plagioclase, calcite, biotite, muscovite, epidote. Fine-grained with somewhat larger calcite crystals; bands rich in epidote and biotite alternated with bands rich in plagioclase, calcite, quartz.
- ET 5 *Biotitic amphibolite.* Amphibole, plagioclase, biotite, calcite, quartz. Medium-grained, calcite in layers parallel to strong orientation of amphiboles and to biotite-rich belts.
- ET 6 *Biotite gneiss.* Biotite, quartz, plagioclase, muscovite. Medium-grained, muscovite well-oriented in bands with fine-grained and elongated quartz which are parallel to belts of medium-grained, granular, fresh quartz; biotite sigmoidal.

- ET 7 *Quartz-amphibole schist*. Quartz, amphibole. Very fine-grained, amphibole oriented parallel to the axial surfaces of microfolds of quartz-rich bands and to bands of medium-grained, fresh, polygonal quartz.
- ET 8 *Biotitic quartzite*. Quartz, biotite. Extremely fine-grained with patches of coarser quartz grains with undulose extinction. Perhaps result of cataclastic deformation.
- ET 9 *Conglomerate*. Limestone pebbles, quartz grains in quartz matrix and recrystallized calcite-quartz veins. Fine-grained very elongated quartz in the pressure shadows of the pebbles.
- ET 11 *Conglomerate*. Same as ET 9.
- ET 12 *Chlorite-epidote schist*. Epidote, calcite, plagioclase, chlorite. Fine-grained, subophytic texture, chlorite abundant along cleavages, calcite lenses.
- ET 13 *Porphyritic gabbrodiorite*. Plagioclase, amphibole, quartz. Medium-grained subophytic texture, idiomorphic matrix, two generations of plagioclase and amphibole.
- ET 14 *Chlorite schist*. Plagioclase, chlorite, calcite. Fine-grained chlorite and plagioclase with larger plagioclase grains and calcite lenses.
- ET 15 *Epidote schist*. Plagioclase, epidote, biotite, chlorite. Fine-grained, altered quartziferous diorite.
- ET 16 *Diorite*. Plagioclase, amphibole. With minor amounts of K-feldspar. Altered.
- ET 17 *Conglomeratic sandstone*. Quartz, plagioclase, sericite. Very fine-grained with somewhat larger quartz grains.
- ET 18 *Phyllite*. Quartz, muscovite, plagioclase, calcite. Fine-grained with calcite inclusions, quartz rather elongated, muscovite crenulated.
- ET 19 *Conglomeratic phyllite*. Quartz, sericite, plagioclase, opaque. Very fine-grained with larger quartz grains.
- ET 20 *Conglomerate*. Quartz, calcite, chlorite. Fine-grained chloritic matrix with quartz and calcite pebbles.
- ET 21 *Quartz-amphibole gneiss*. Quartz, amphibole, epidote, calcite, plagioclase, garnet. Medium-grained with quartz in bands elongated in a direction not parallel to the compositional banding; calcite in veins not parallel to other planar elements; plagioclase larger, roundish, with inclusions.
- ET 22 *Phyllitic quartzite*. Quartz, sericite, calcite. Medium-grained, with bands of sericite parallel to the axial surfaces of microfolds; quartz elongated and calcite in veins.
- ET 23 *Quartziferous phyllite*. Quartz, sericite, biotite, muscovite, plagioclase, calcite, tourmaline. Fine-grained with quartz somewhat elongated, calcite in veins.
- ET 25 *Amphibolite*. Amphibole, plagioclase. Fine-grained with roundish remnants of larger plagioclase in a plagioclase-amphibole groundmass.
- ET 26 *Dolerite*. Amphibole, plagioclase, chlorite, apatite. Medium-grained with zoned plagioclase idiomorphic, sericitized; amphibole also zoned.
- ET 27 *Biotite-muscovite gneiss*. Quartz, plagioclase, muscovite, biotite, K-feldspar. Medium-grained with biotite in bundles. No retrometamorphism.
- ET 28 *Biotite-epidote gneiss*. Quartz, plagioclase, biotite, epidote, muscovite. Fine-grained with "rotated" blasts.
- ET 29 *Biotite-epidote gneiss*. Quartz, biotite, epidote, muscovite, plagioclase, K-feldspar. Fine-grained with two preferential orientations of elongated minerals; quartz polygonal.
- ET 30 *Quartz-chlorite phyllite*. Quartz, plagioclase, chlorite. Very fine-grained with texture of probably volcanic origin.
- ET 31 *Quartz-amphibole phyllite*. Quartz, tremolite, hornblende, epidote. Very fine-grained.
- ET 32 *Biotite-amphibole gneiss*. Quartz, plagioclase, biotite, tremolite, hornblende. Fine-grained, banded, schistose.
- ET 33 *Gabbrodiorite*. Plagioclase, pyroxene. Coarse-grained. Fresh and undeformed.